

Synthesis and Structure of Formally Hexavalent Palladium Complexes

Wanzhi Chen, Shigeru Shimada,* Masato Tanaka*

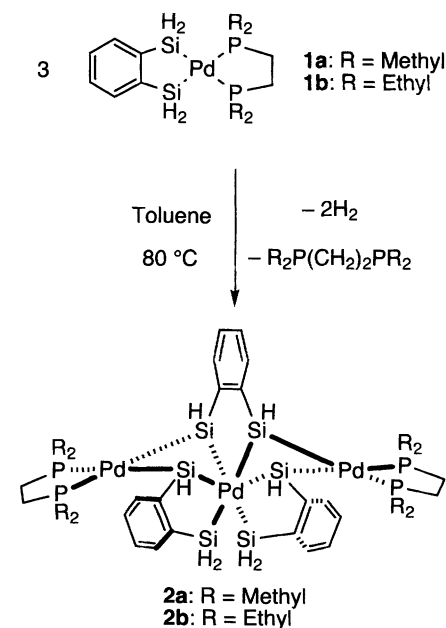
Formally hexavalent palladium complexes have been isolated and structurally characterized for the first time. Thermal condensation reaction of three molecules of 1,2- $C_6H_4(SiH_2)_2Pd^{II}(R_2PCH_2CH_2PR_2)$ (where R is defined as a methyl or ethyl) provided trinuclear palladium complexes. Single-crystal x-ray analysis revealed that each of the central palladium atoms of the complexes is ligated by six silicon atoms and is hexavalent, whereas the other palladium atoms are divalent.

The highest oxidation state theoretically attainable for an element is the total number of valence shell electrons. However, most transition metals of group 8 or later cannot attain their maximum oxidation states (1, 2). For group 10 metals (platinum, palladium, and nickel), the highest oxidation state known in an isolable compound is metal(VI) and is attained only for platinum as $Pt^{VI}F_6$, which was first synthesized in 1957 (3) and has been the subject of many experimental and theoretical studies (4–6). High-oxidation-state compounds are generally less stable for the elements of the first and second transition series than those of the third transition series, and no structurally characterized metal(V) and metal(VI) complexes are known for palladium and nickel (1, 2), although electrochemical formation of $Pd^{VI}O_3$ has been discussed (7, 8).

Palladium is one of the most versatile transition metal catalysts for the transformation of organic and heteroatom compounds as well as for the treatment of vehicle exhaust gas. Although palladium generally prefers lower oxidation states (Pd^0 or Pd^{II}) (9), recent studies showed the importance of a higher oxidation state (Pd^{IV}) in catalytic processes (10, 11). The highest-oxidation-state compounds of transition metals are often attained with highly electronegative ligands, such as fluorides or oxides, for example, PtF_6 , IrF_6 , RhF_6 , OsO_4 , and RuO_4 (1, 6). Recently, several examples of high-oxidation-state complexes with silyl ligands, which are more electropositive than fluoride or oxide ligands, have been reported (12–15), although the oxidation states in these complexes are rather formal ones because M–Si (where M–metal) bond is much less ionic than M–F and M–O bonds. We also have found that a bidentate silyl ligand can sta-

bilize silyl complexes of Pt^{IV} , Pd^{IV} , and Ni^{IV} , which are unusually thermally stable (16–19). On the basis of these results, we designed a new tridentate silyl ligand (20) to attain higher-oxidation-state silyl transition-metal complexes. Although the attempt to obtain a hexavalent silylplatinum complex by using the tridentate silyl ligand was not successful (21), we succeeded unexpectedly in isolating formally hexavalent palladium complexes as trinuclear ones by the trimerization reaction of Pd^{II} complexes bearing the bidentate silyl ligand.

The trinuclear palladium complex **2a** was obtained by the condensation reaction of three molecules of palladium complex, 1,2- $C_6H_4(SiH_2)_2Pd^{II}(dmpe)$ **1a** [where $dmpe = 1,2$ -bis(dimethylphosphino)ethane], in toluene at 80°C for 2 days (Scheme 1) (22). Complex **2a** was isolated as red crystals in 28% yield from the reaction mixture by keeping the mixture at room temperature. Com-



Scheme 1. Synthesis of trinuclear complexes **2a** and **2b**.

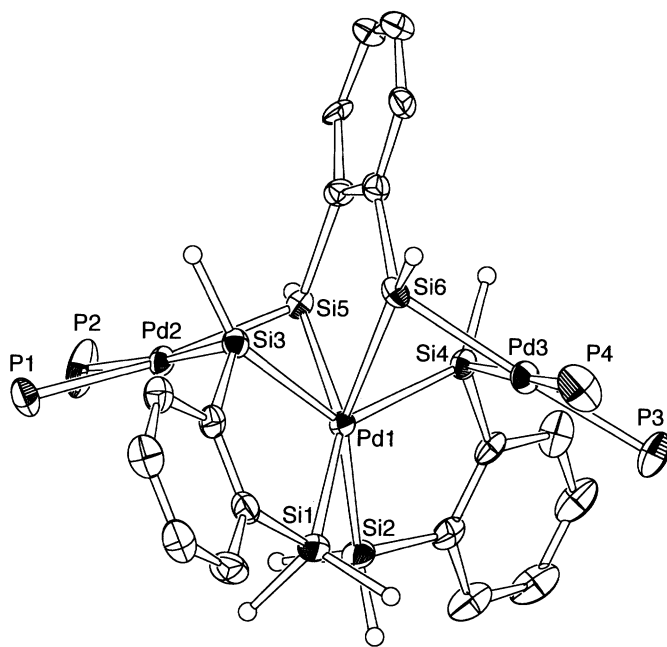
15. J.-Y. Cho, C. N. Iverson, M. R. Smith III, *J. Am. Chem. Soc.* **122**, 12868 (2000).
16. K. Kawamura, J. F. Hartwig, *J. Am. Chem. Soc.* **123**, 8422 (2001).
17. At 150°C, the following isomer ratios were obtained for anisole borylation with 20 mol% precatalyst loadings: Cp^*IrH_4 , $o:m:p = 3:49:48$; **1**, $o:m:p = 2:79:19$.
18. Compound **4** has been prepared as an analytically pure white solid. Relevant spectroscopic data include: 1H NMR (C_6D_6) δ 1.33 (s, 36 H, $BO_2C_6H_{12}$), 2.23 (s, 9 H, $C_6H_3(CH_3)_3$), 5.62 (s, 3 H, $C_6H_3(CH_3)_3$); ^{11}B NMR (C_6D_6) δ 32.5; ^{13}C NMR (C_6D_6) δ 19.68, 25.73, 80.95, 96.97, 118.05.
19. Compound **3** is synthesized in 86% yield from indenyl lithium and $[IrCl(COD)]_2$ [J. S. Merola, R. T. Kacmarcik, *Organometallics* **8**, 778 (1989)].
20. For catalysts generated from 4 mol% PMe_3 and 2 mol% **3** or **4**, isomer ratios were obtained for anisole borylation at 150°C as follows: **3**, $o:m:p = 9:74:17$; **4**, $o:m:p = 8:75:17$. For **3** and **4**, ortho borylation increases slightly, which could signify a minor pathway that is not accessible from **1**.
21. A Rh catalyst that is highly selective for benzylic borylation has been recently reported [S. Shimada, A. S. Batsanov, J. A. K. Howard, T. B. Marder, *Angew. Chem. Int. Ed. Engl.* **40**, 2168 (2001)].
22. A representative procedure for borylation is given for entry 10 of Fig. 2. In a glove box under N_2 , compound **3** (57 mg, 0.14 mmol) and $dppe$ (54 mg, 0.14 mmol) were dissolved in HBPIn (1.30 g, 10.2 mmol). The solution was transferred to a thick-walled air-free flask containing 1,3-dichlorobenzene (1.00 g, 6.80 mmol). The clear yellow solution was heated at 100°C under N_2 and monitored by GC-flame ionization detection (GC-FID). After 14 hours, the reaction mixture was pumped down to obtain a brown oil, which was vacuum distilled at 93° to 94°C (0.03 mm Hg). The resulting oil was then dissolved in Et_2O (10 ml) and washed with H_2O (5×100 ml). After drying over $MgSO_4$, ether was removed under high vacuum to give 1.65 g (89% yield) of colorless 1,3,5- $C_6H_3Cl_2BPin$ (melting point, 36° to 38°C). NMR values are as follows: 1H (500 MHz, $CDCl_3$) δ 1.32 (s, 12 H), 7.41 (t, $J = 2.0$ Hz, 1 H), 7.63 (d, $J = 2.0$ Hz, 2 H); ^{13}C (125 MHz, $CDCl_3$) δ 24.82, 84.49, 131.1, 133.7, 134.7; ^{11}B ($CDCl_3$) δ 30.
23. Dechlorination was observed during attempted silylations of 1,3-dichlorobenzene with the use of closely related Rh catalysts [K. Ezbiansky *et al.*, *Organometallics* **17**, 1455 (1998)].
24. M. Murata, T. Oyama, S. Watanabe, Y. Masuda, *J. Org. Chem.* **65**, 164 (2000).
25. M. K. Tse, J.-Y. Cho, M. R. Smith III, *Org. Lett.* **3**, 2831 (2001).
26. For a Zr-Pd catalyzed route to substituted biphenyls and terphenyls, see M. Frid, D. Pérez, A. J. Peat, S. L. Buchwald, *J. Am. Chem. Soc.* **121**, 9469 (1999).
27. Y. H. Kim, O. W. Webster, *Macromolecules* **25**, 5561 (1992).
28. For the material in Fig. 3B, the weight-average molecular weight $M_w = 6374$ and the number-average molecular weight $M_n = 3460$, compared with the previously reported values of $M_w = 5750$ and $M_n = 3820$ (27).
29. Compounds **6** and **7** have been fully characterized, and details will be reported separately. The following spectroscopic data are included: **6**, 1H NMR (C_6D_6 , 25°C) δ 1.24 (s, 12H), 1.58 (b, 36H); ^{11}B NMR (C_6D_6) δ 38; $^{31}P\{^1H\}$ NMR (C_6D_6) δ -57.5; **7**, 1H NMR (C_6D_6) δ 1.34 (s, 36 H), 1.52 (m, 27 H); ^{11}B NMR (C_6D_6) δ 36.0; $^{31}P\{^1H\}$ NMR (C_6D_6) δ -64.
30. We thank A. Odom for stimulating discussions and C. Radano for assistance with polymer characterization. Supported by the NIH-NIGMS (grant R01 GM63188-01 to M.R.S.), the NSF (grant CHE-9817230 to M.R.S.), the Michigan Life Sciences Corridor Fund (to R.E.M. and M.R.S.), and the Yamanouchi USA Foundation (to D.H. and R.E.M.).

12 October 2001; accepted 13 November 2001
 Published online 22 November 2001;
 10.1126/science.1067074
 Include this information when citing this paper.

National Institute of Advanced Industrial Science and Technology (AIST), Tsukuba Central 5, 1-1-1 Higashi, Tsukuba, Ibaraki 305-8565, Japan.

*To whom correspondence should be addressed. E-mail: s-shimada@aist.go.jp (S.S.); m.tanaka@aist.go.jp (M.T.)

Fig. 1. Molecular structure of complex **2a** (30% probability ellipsoids for Pd, Si, P, and C). Carbon atoms on the phosphorous atoms and hydrogen atoms on the carbon atoms are omitted for clarity. Selected bond lengths in Å are as follows: Pd1–Si1, 2.348(3); Pd1–Si2, 2.353(3); Pd1–Si3, 2.493(3); Pd1–Si4, 2.440(3); Pd1–Si5, 2.437(3); Pd1–Si6, 2.562(3); Pd2–Si3, 2.376(3); Pd2–Si5, 2.414(3); Pd3–Si4, 2.373(3); Pd3–Si6, 2.390(3). Selected bond angles in degrees are as follows: Pd2–Pd1–Pd3, 147.05(4); Si1–Pd1–Si2, 74.0(1); Si1–Pd1–Si3, 83.9(1); Si2–Pd1–Si4, 84.4(1); Si3–Pd1–Si5, 82.51(9); Si3–Pd1–Si6, 58.95(9); Si4–Pd1–Si5, 64.14(9); Si4–Pd1–Si6, 79.41(9); Si5–Pd1–Si6, 83.2(1); P1–Pd2–P2, 85.4(1); Si3–Pd2–Si5, 85.50(9); P3–Pd3–P4, 86.4(2); Si4–Pd3–Si6, 84.3(1); Pd1–Si3–Pd2, 72.82(8); Pd1–Si4–Pd3, 74.44(9); Pd1–Si5–Pd2, 73.15(9); Pd1–Si6–Pd3, 71.93(9).



plex **2b** was similarly obtained from **1b** in 45% yield after purification by alumina column chromatography under N_2 atmosphere (22). The structures of **2a** and **2b** were unambiguously determined by the single-crystal x-ray structure analysis (for **2b**, two independent molecules were found in a unit cell) and were proved to be similar to each other (Fig. 1) (23). The structural features of **2a** and **2b** are as follows. The central palladium atom Pd1 (the atomic numbering refers to that in Fig. 1) no longer retains the chelating phosphine ligand but instead is ligated by six Si atoms to form a formal Pd^{VI} center. The geometry of Pd1 is highly distorted probably because of the presence of two peripheral Pd atoms. Each of the peripheral Pd atoms is divalent and is connected to the central Pd atom via two Si bridges to form spiro[3.3]heptane framework. The geometries of the peripheral Pd atoms are typical square planar. Two Pd1–SiH₂ bond lengths [average 2.351(3) Å for **2a** and 2.356(3) Å for **2b**, where the numbers in parentheses are the errors in the last digit] and Pd2–SiH and Pd3–SiH bond lengths [2.373(3) to 2.414(3) Å, average 2.388(3) Å for **2a**; 2.371(2) to 2.409(3) Å, average 2.384(3) Å for **2b**] are comparable to the known Pd–Si bond lengths [2.318(2) Å to 2.411(2) Å] (14, 17, 24–30), whereas four Pd1–SiH bond lengths [2.437(3) to 2.562(3) Å, average 2.483(3) Å for **2a**; 2.420(3) to 2.521(2) Å, average 2.468(2) Å for **2b**] are considerably longer than those. Distances Pd1–Pd2 and Pd1–Pd3 [average 2.902(2) Å for **2a** and 2.9158(8) Å for **2b**] are longer than those in other related silapalladacycles [2.691(1) to 2.751(3) Å] (14, 29, 30).

Another interesting structural feature of **2a** and **2b** is the short Si–Si contact between Si3 and Si6, and Si4 and Si5 [average of Si3–Si6 and Si4–Si5 distances, 2.539(4) Å for **2a** and 2.551(3) Å for **2b**]. It is not clear whether the short contacts simply come from the steric requirement or whether any bonding interaction exists between these Si atoms. If Si–Si bonds are assumed between these Si atoms, central Pd atoms of **2a** and **2b** are not Pd^{VI} but can be described as bis σ -complexes of Pd^{II} with Si–Si bonds (Fig. 2) (31); this is an equally unprecedented situation. The best choice of bonding model will need further work for full clarification.

Nuclear magnetic resonance (NMR) and infrared (IR) spectra of **2a** and **2b** were consistent with their solid state structures and suggested the absence of agostic Si–H bonds or a neutral H₂ ligand, which might escape detection by X-ray analysis (32). ²⁹Si NMR spectrum of **2b** showed two SiH and one SiH₂ signals with normal J_{H-Si} values (182–187 Hz, J is the spin-spin coupling constant). No dynamic behavior was observed in ¹H, ³¹P and ²⁹Si NMR spectroscopies of **2b** at the temperature ranging from –80 to +50 °C. IR spectrum of **2b** showed intense Si–H stretching absorption at 2038 cm^{–1} and no absorption assignable to agostic Si–H bonds or a neutral H₂ ligand.

The formation of **2a** and **2b** is in contrast to the condensation reactions of a Pt complex 1,2-C₆H₄(SiH₂)₂Pt^{II}(PEt₃)₂ **3** and Ni complexes 1,2-C₆H₄(SiH₂)₂Ni^{II}(R₂PCH₂CH₂PR₂) **4** (R = Me or Et) similar to **1a** and **1b**. Complexes **3** and **4** dimerized to form a dinuclear, mixed valent Pt^{III}Pt^{IV} complex **5** (16) and dinuclear Ni^{III} complexes **6** (33), respectively (Fig. 3). Further study is necessary to clarify

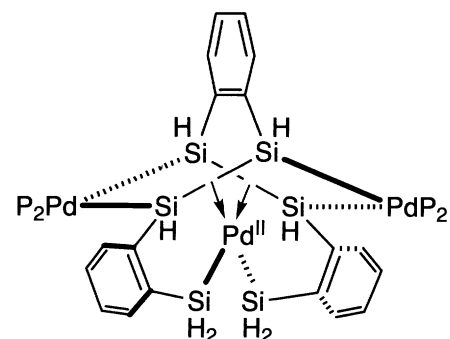


Fig. 2. Alternative description of complexes **2a** and **2b** (P_2 = dmpe or depe).

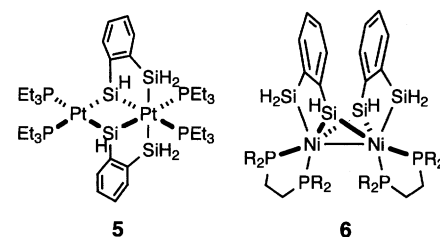


Fig. 3. Dinuclear Pt complex **5** and Ni complex **6**.

the mechanism of the formation of complexes **2a** and **2b** as well as the differences in the products among Ni, Pd, and Pt.

PtF₆, the only structurally characterized Pt^{VI} compound, has highly electronegative F atoms, whereas the formally hexavalent Pd atoms of **2a** and **2b** are ligated by six Si atoms, which are much more electropositive than F. This result suggests a variety of elements can serve as ligands for hexavalent group 10 metal compounds as well as for other high-oxidation-state transition-metal compounds. We believe that high-oxidation-state transition-metal species ligated by heteroatoms will be much more important than expected in the transition-metal catalyzed transformation of heteroatom compounds, which has become increasingly important and will provide new methodologies for the construction of materials based on heteroatoms (34).

References and Notes

- F. A. Cotton, G. Wilkinson, C. A. Murillo, M. Bochmann, *Advanced Inorganic Chemistry* (Wiley, New York, ed. 6, 1999), chaps. 16–18.
- R. H. Crabtree, *The Organometallic Chemistry of The Transition Metals* (Wiley, New York, ed. 2, 1994), chap. 15.
- B. Weinstock, H. H. Claassen, J. G. Malm, *J. Am. Chem. Soc.* **79**, 5832 (1957).
- A. K. Brisdon *et al.*, *J. Chem. Soc. Dalton Trans.* **1992**, 139 (1992).
- R. Marx, K. Seppelt, R. M. Ibberson, *J. Chem. Phys.* **104**, 7658 (1996).
- R. Wesendorf, P. Schwerdtfeger, *Inorg. Chem.* **40**, 3351 (2001).
- L. D. Burke, J. K. Casey, *J. Electrochem. Soc.* **140**, 1284 (1993).
- M.-C. Jeong, C. H. Pyun, I.-H. Yeo, *J. Electrochem. Soc.* **140**, 1986 (1993).

9. J. Tsuji, *Palladium Reagents and Catalysts* (Wiley, Chichester, UK, 1995).

10. A. J. Canty, *Acc. Chem. Res.* **25**, 83 (1992).

11. C. J. Elsevier, *Coord. Chem. Rev.* **185-186**, 809 (1999).

12. M.-J. Fernandez, P. M. Maitlis, *J. Chem. Soc. Chem. Commun.* **1982**, 310 (1982).

13. J. Y. Corey, J. Braddock-Wilking, *Chem. Rev.* **99**, 175 (1999).

14. M. Suginome, Y. Kato, N. Takeda, H. Oike, Y. Ito, *Organometallics* **17**, 495 (1998).

15. M. Brookhart, B. E. Grant, C. P. Lenges, M. H. Prosenc, P. S. White, *Angew. Chem. Int. Ed.* **39**, 1676 (2000).

16. S. Shimada, M. Tanaka, K. Honda, *J. Am. Chem. Soc.* **117**, 8289 (1995).

17. S. Shimada, M. Tanaka, M. Shiro, *Angew. Chem. Int. Ed. Engl.* **35**, 1856 (1996).

18. S. Shimada, M. L. N. Rao, M. Tanaka, *Organometallics* **18**, 291 (1999).

19. Ir^Y complexes with bidentate silyl ligands were also reported [M. Loza, J. W. Faller, R. H. Crabtree, *Inorg. Chem.* **34**, 2937 (1995)].

20. W. Chen, S. Shimada, T. Hayashi, M. Tanaka, *Chem. Lett.* **2001**, 1096 (2001).

21. W. Chen, S. Shimada, M. Tanaka, unpublished data.

22. Details of synthetic procedure for complexes **1a**, **1b**, **2a**, and **2b** and NMR data for **1a** and **1b** are available at Science Online (35).

23. X-ray crystallographic analysis was carried out on a Rigaku AFC7R diffractometer using a rotating anode (58 kV, 280 mA for **2a** and 56 kV, 270 mA for **2b**) with graphite monochromated Mo-K_α radiation ($\lambda = 0.71069 \text{ \AA}$). Crystal data for **2a**: C₃₀H₅₂P₄Pd₃Si₆; MW = 1024.35; orthorhombic; space group Fdd2; Z = 16; T = -100° ± 1°C; a = 18.524(9) Å, b = 76.981(5) Å, c = 11.964(3) Å, and V = 17060(8) Å³; goodness of fit = 1.05; R [I > 2σ(I)] = 0.040; wR2 = 0.117 (all data). Crystal data for **2b**: C₃₈H₆₈P₄Pd₃Si₆; MW = 1136.56; triclinic; space group P-1; Z = 4; T = -80° ± 1°C; a = 20.051(2) Å, b = 21.546(3) Å, c = 11.565(1) Å, α = 90.199(10)°, β = 97.188(8)°, γ = 87.893(10)°, and V = 4953.6(10) Å³; goodness of fit = 1.89; R [I > 2σ(I)] = 0.065; wR2 = 0.206 (all data). Atomic coordinates, bond lengths, and angles and the other important parameters have been deposited with the Cambridge Crystallographic Data Centre as supplementary publications CCDC 174451 and 174452. Copies of the data can be obtained, free of charge, from CCDC (e-mail: deposit@ccdc.cam.ac.uk). Details of x-ray crystallographic analysis are also available at Science Online (35).

24. Y. Pan, J. T. Mague, M. J. Fink, *Organometallics* **11**, 3495 (1992).

25. M. Murakami, T. Yoshida, Y. Ito, *Organometallics* **13**, 2900 (1994).

26. M. Suginome, H. Oike, P. H. Shuff, Y. Ito, *Organometallics* **15**, 2170 (1996).

27. M. Suginome, H. Oike, S.-S. Park, Y. Ito, *Bull. Chem. Soc. Jpn.* **69**, 289 (1996).

28. Y. Tanaka, H. Yamashita, S. Shimada, M. Tanaka, *Organometallics* **16**, 3246 (1997).

29. Y.-J. Kim et al., *Organometallics* **17**, 4929 (1998).

30. Y.-J. Kim et al., *J. Chem. Soc. Dalton Trans.* **2000**, 417 (2000).

31. R. H. Crabtree, *Angew. Chem. Int. Ed. Engl.* **32**, 789 (1993).

32. NMR of **2a** ([D₆]benzene solution, ¹H) δ value (parts per million) 0.40 (doublet, 6H, J_{p-h} = 7 Hz); 0.65 to 1.05 (multiplet, 8H); 0.78 (doublet, 6H, J_{p-h} = 7 Hz); 0.89 (doublet, 6H, J_{p-h} = 7 Hz); 1.00 (doublet, 6H, J_{p-h} = 7 Hz); 4.30 (broad singlet, 2H); 5.00 to 5.20 [a sharp doublet (J = 20 Hz) and a broad multiplet are overlapped, 6H]; 8.03 to 8.08 (multiplet, 4H); 8.25 (doublet of doublet, 2H, J_{h-h} = 3 and 5 Hz). Because of the low solubility of **2a**, signals for a part of aromatic hydrogens (6H) laid under the signals of the residual hydrogen signals of the solvent. ([D₆]benzene solution, ³¹P) δ value, 21.1 (doublet, J_{p-p} = 24 Hz); 21.4 (doublet, J_{p-p} = 24 Hz). ²⁹Si NMR spectrum of **2a** was not obtained due to the low solubility of **2a**. NMR of **2b** ([D₆]toluene solution, ¹H) δ value, 0.7 to 1.7 (multiplet, 44H); 1.72 to 1.83 (multiplet, 2H); 1.93 to 2.04 (multiplet, 2H); 4.16 (broad singlet, 2H); 5.18 to

5.73 [a sharp doublet (J = 12 Hz) and a broad multiplet are overlapped, 6H]; 7.33 to 7.43 (multiplet, 6H); 8.18 (doublet, 2H, J_{h-h} = 6 Hz); 8.22 (doublet, 2H, J_{h-h} = 6 Hz); 8.35 (doublet of doublet, 2H, J_{h-h} = 3 and 5 Hz); ([D₆]toluene solution, ³¹P) δ value, 48.5 (doublet, J_{p-p} = 24 Hz); 48.8 (doublet, J_{p-p} = 24 Hz); ([D₆]toluene solution, ²⁹Si) δ value, -12.9 [doublet of doublet, J_{p-si} = 22 and 124 Hz, (J_{h-si} = 182 Hz)], SiH; -11.3 [singlet, (J_{h-si} = 184 Hz)], SiH₂; 20.0 [doublet of doublet of doublet, J_{p-si} = 5, 23 and 111 Hz, (J_{h-si} = 187 Hz)], SiH. ¹H-decoupled and ¹H-coupled ²⁹Si NMR spectra were measured. The J_{p-si} values were obtained from ¹H-decoupled spectrum and the number of hydrogen atoms bound to the silicon atoms and the J_{h-si} values were determined by ¹H-coupled spectrum. IR of **2b** (KBr pellet) 3033, 2960, 2927, 2898, 2871, 2038, 1454,

1413, 1376, 1238, 1099, 1025, 944, 865, 794, 757, 682, 626, and 449 cm⁻¹.

33. S. Shimada, M. L. N. Rao, T. Hayashi, M. Tanaka, *Angew. Chem. Int. Ed.* **40**, 213 (2001).

34. L.-B. Han, M. Tanaka, *Chem. Commun.* **1999**, 395 (1999).

35. Supplementary data are available on Science Online at www.sciencemag.org/cgi/content/full/295/5553/308/DC1.

36. We are grateful to the Japan Science and Technology Corporation (JST) for financial support through the CREST (Core Research for Evolutional Science and Technology) program and for a postdoctoral fellowship (to W.C.).

11 October 2001; accepted 28 November 2001

Direct Determination of the Timing of Sea Level Change During Termination II

Christina D. Gallup,^{1*} H. Cheng,² F. W. Taylor,³ R. L. Edwards²

An outcrop within the last interglacial terrace on Barbados contains corals that grew during the penultimate deglaciation, or Termination II. We used combined ²³⁰Th and ²³¹Pa dating to determine that they grew 135.8 ± 0.8 thousand years ago, indicating that sea level was 18 ± 3 meters below present sea level at the time. This suggests that sea level had risen to within 20% of its peak last-interglacial value by 136 thousand years ago, in conflict with Milankovitch theory predictions. Orbital forcing may have played a role in the deglaciation, as may have isostatic adjustments due to large ice sheets. Other corals in the same outcrop grew during oxygen isotope (δ¹⁸O) substage 6e, indicating that sea level was 38 ± 5 meters below present sea level, about 168.0 thousand years ago. When compared to the δ¹⁸O signal in the benthic V19-30/V19-28 record at that time, the coral data extend to the previous glacial cycle the conclusion that deep-water temperatures were colder during glacial periods.

The timing of the penultimate deglaciation (Termination II) has fundamental implications for the causes of climate change. Terminations, as distinct climatic events, provide an opportunity to test the Milankovitch theory of orbital forcing of the glacial cycles, which holds that increases in summer insolation at high Northern latitudes should precede or coincide with glacial melting and, similarly, that decreases should precede or coincide with glacial growth. However, despite decades of studies aimed at constraining the timing of sea level change during Termination II, the question of whether its timing is consistent with Milankovitch theory predictions remains unanswered. As direct indicators of sea level, corals are a potential resource for addressing the problem. The main hurdles

have been: (i) finding corals that record sea level during Termination II and (ii) demonstrating that uranium-series ages have remained unchanged by the effects of diagenesis. We have identified Termination II corals on Barbados and have tested them for diagenesis using combined ²³⁰Th and ²³¹Pa dating.

Two efforts to date Termination II, from Devils Hole, in Nevada, United States (1) and Bahamian coastal sediments (2), suggest that the deglaciation occurred too early to have been caused directly by orbital forcing. ²³⁰Th dating of the Devils Hole calcite vein isotopic oxygen (δ¹⁸O) record (3, 4) places the midpoint of the δ¹⁸O rise during Termination II at 140 ± 3 thousand years ago (ka), 6 ± 3 thousand years before the midpoint in the rise of 65°N summer insolation. U-Th isochron dating of carbonate sediments from the slopes of the Bahamas places the midpoint of the marine δ¹⁸O rise at 135 ± 2.5 ka (2), within error of the midpoint of the rise in 65°N summer insolation. Although these data are compelling, questions remain (5) because neither record is a direct measure of sea level.

¹Department of Geological Sciences, University of Minnesota Duluth, Duluth, MN 55812, USA. ²Minnesota Isotope Laboratory, Department of Geology and Geophysics, University of Minnesota, Minneapolis, MN 55455, USA. ³Institute for Geophysics, University of Texas at Austin, Austin, TX 78712, USA.

*To whom correspondence should be addressed. E-mail: cgallup@d.umn.edu